












TECH BRIEFS

NATIONAL AERONAUTICS AND SPACE ADMINISTRATION

-  **Technology Focus**
-  **Electronics/Computers**
-  **Software**
-  **Materials**
-  **Mechanics/Machinery**
-  **Manufacturing**
-  **Bio-Medical**
-  **Physical Sciences**
-  **Information Sciences**
-  **Books and Reports**

INTRODUCTION

Tech Briefs are short announcements of innovations originating from research and development activities of the National Aeronautics and Space Administration. They emphasize information considered likely to be transferable across industrial, regional, or disciplinary lines and are issued to encourage commercial application.

Availability of NASA Tech Briefs and TSPs

Requests for individual Tech Briefs or for Technical Support Packages (TSPs) announced herein should be addressed to

National Technology Transfer Center

Telephone No. (800) 678-6882 or via World Wide Web at www.nttc.edu

Please reference the control numbers appearing at the end of each Tech Brief. Information on NASA's Innovative Partnerships Program (IPP), its documents, and services is also available at the same facility or on the World Wide Web at <http://ipp.nasa.gov>.

Innovative Partnerships Offices are located at NASA field centers to provide technology-transfer access to industrial users. Inquiries can be made by contacting NASA field centers listed below.

NASA Field Centers and Program Offices

Ames Research Center

Lisa L. Lockyer
(650) 604-1754
lisa.l.lockyer@nasa.gov

Dryden Flight Research Center

Gregory Poteat
(661) 276-3872
greg.poteat@dfrc.nasa.gov

Glenn Research Center

Kathy Needham
(216) 433-2802
kathleen.k.needham@nasa.gov

Goddard Space Flight Center

Nona Cheeks
(301) 286-5810
nona.k.cheeks@nasa.gov

Jet Propulsion Laboratory

Ken Wolfenbarger
(818) 354-3821
james.k.wolfenbarger@jpl.nasa.gov

Johnson Space Center

Michele Brekke
(281) 483-4614
michele.a.brekke@nasa.gov

Kennedy Space Center

David R. Makufka
(321) 867-6227
david.r.makufka@nasa.gov

Langley Research Center

Martin Waszak
(757) 864-4015
martin.r.waszak@nasa.gov

Marshall Space Flight Center

Jim Dowdy
(256) 544-7604
jim.dowdy@msfc.nasa.gov

Stennis Space Center

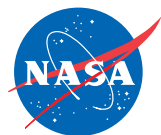
John Bailey
(228) 688-1660
john.w.bailey@nasa.gov

Carl Ray, Program Executive

Small Business Innovation
Research (SBIR) & Small
Business Technology
Transfer (STTR) Programs
(202) 358-4652
carl.g.ray@nasa.gov

Doug Comstock, Director

Innovative Partnerships
Program Office
(202) 358-2560
doug.comstock@nasa.gov



TECH BRIEFS

NATIONAL AERONAUTICS AND SPACE ADMINISTRATION



5 Technology Focus: Communications

- 5 High-Accuracy, High-Dynamic-Range Phase-Measurement System
- 5 Simple, Compact, Safe Impact Tester
- 6 Multi-Antenna Radar Systems for Doppler Rain Measurements
- 7 600-GHz Electronically Tunable Vector Measurement System
- 8 Modular Architecture for the Measurement of Space Radiation



11 Electronics/Computers

- 11 VLSI Design of a Turbo Decoder
- 12 Architecture of an Autonomous Radio Receiver
- 13 Improved On-Chip Measurement of Delay in an FPGA or ASIC



15 Software

- 15 Resource Selection and Ranking
- 15 Accident/Mishap Investigation System



17 Bio-Medical

- 17 Simplified Identification of mRNA or DNA in Whole Cells
- 17 Printed Multi-Turn Loop Antennas for RF Biotelemetry



19 Materials

- 19 Making Ternary Quantum Dots From Single-Source Precursors
- 19 Improved Single-Source Precursors for Solar-Cell Absorbers
- 20 Spray CVD for Making Solar-Cell Absorber Layers
- 21 Glass/BNNT Composite for Sealing Solid Oxide Fuel Cells



23 Manufacturing & Prototyping

- 23 A Method of Assembling Compact Coherent Fiber-Optic Bundles
- 23 Manufacturing Diamond Under Very High Pressure



25 Physical Sciences

- 25 Ring-Resonator/Sol-Gel Interferometric Immunosensor
- 25 Compact Fuel-Cell System Would Consume Neat Methanol



29 Information Sciences

- 29 Algorithm Would Enable Robots to Solve Problems Creatively
- 30 Hypothetical Scenario Generator for Fault-Tolerant Diagnosis



31 Books & Reports

- 31 Smart Data Node in the Sky
- 31 Pseudo-Waypoint Guidance for Proximity Spacecraft Maneuvers
- 31 Update on Controlling Herds of Cooperative Robots
- 31 Simulation and Testing of Maneuvering of a Planetary Rover

This document was prepared under the sponsorship of the National Aeronautics and Space Administration. Neither the United States Government nor any person acting on behalf of the United States Government assumes any liability resulting from the use of the information contained in this document, or warrants that such use will be free from privately owned rights.



High-Accuracy, High-Dynamic-Range Phase-Measurement System

Phase differences can be measured to within a microcycle.

NASA's Jet Propulsion Laboratory, Pasadena, California

A digital phase meter has been designed to satisfy stringent requirements for measuring differences between phases of radio-frequency (RF) subcarrier signals modulated onto laser beams involved in the operation of a planned space-borne gravitational-wave-detecting heterodyne laser interferometer. The capabilities of this system could also be used in diverse terrestrial applications that involve measurement of signal phases, including metrology, navigation, and communications. The capabilities of this system include:

- Accuracy to within a millionth of a cycle (greater than the accuracy of any prior phase meter);
- High dynamic range of phase (limited only by numerical capabilities of a supporting computer);
- Wide input frequency range (≈ 10 kHz to ≈ 20 MHz),
- Maintenance of accuracy even when the frequency of a signal slews by as much as 700 kHz/s within this range; and
- The ability to distinguish and measure multiple tones on the same carrier with undiminished accuracy.

In the operation of this system, two RF modulated laser beams interfere on a photodiode; their frequency difference results in a RF heterodyne signal. The

RF signal output by the photodiode is digitized at 40 Mega-samples/s, then fed into a field-programmable gate array (FPGA). The digitized heterodyne signal is split and multiplied by two adjustable local oscillators (LOs), which separates the signal into in-phase (I) cosine and a quadrature phase (Q) sine components. During stable operation at a small phase difference between the RF and LO signals, the Q multiplier output includes a low-frequency component proportional to the phase difference. This phase-difference output is used to update the LO frequency (and, thereby, the LO phase) to keep the local oscillators locked to the incoming signal. The tracking loop updates the LO frequency every 0.1 ms.

While this makes for a stable digital phase-locked loop, to achieve the desired micro-cycle phase accuracy, the residual phase-tracking error is combined with the LO phase. The residual phase difference is computed as the arctangent of the ratio between the Q and I signals, filtered appropriately, and added to the phase used to update the local oscillators.

For transmission to ground, the phase measurements are decimated from 40 MHz to the frequency-and-phase-update

rate of 10 kHz, then again to a final output rate of 100 Hz. To suppress aliasing of noise in the signal band from 1 mHz to 1 Hz in the decimation from 40 MHz to 10 kHz, an anti-aliasing filter is applied prior to decimation. After the reconstruction of phase at 10 kHz and prior to the final decimation to 100 Hz, another finite-impulse-response anti-aliasing decimation filter is applied. The characteristics of the antialiasing filters are tailored to the phase noise of the input signal.

This work was done by Daniel Shaddock, Brent Ware, Peter Halverson, and Robert Spero of Caltech for NASA's Jet Propulsion Laboratory. Further information is contained in a TSP (see page 1).

In accordance with Public Law 96-517, the contractor has elected to retain title to this invention. Inquiries concerning rights for its commercial use should be addressed to:

*Innovative Technology Assets Management
JPL*

*Mail Stop 202-233
4800 Oak Grove Drive
Pasadena, CA 91109-8099
(818) 354-2240*

E-mail: iaoffice@jpl.nasa.gov

Refer to NPO-41927, volume and number of this NASA Tech Briefs issue, and the page number.

Simple, Compact, Safe Impact Tester

Cushioned impact decelerations up to hundreds of normal Earth gravitation are easily produced.

Ames Research Center, Moffett Field, California

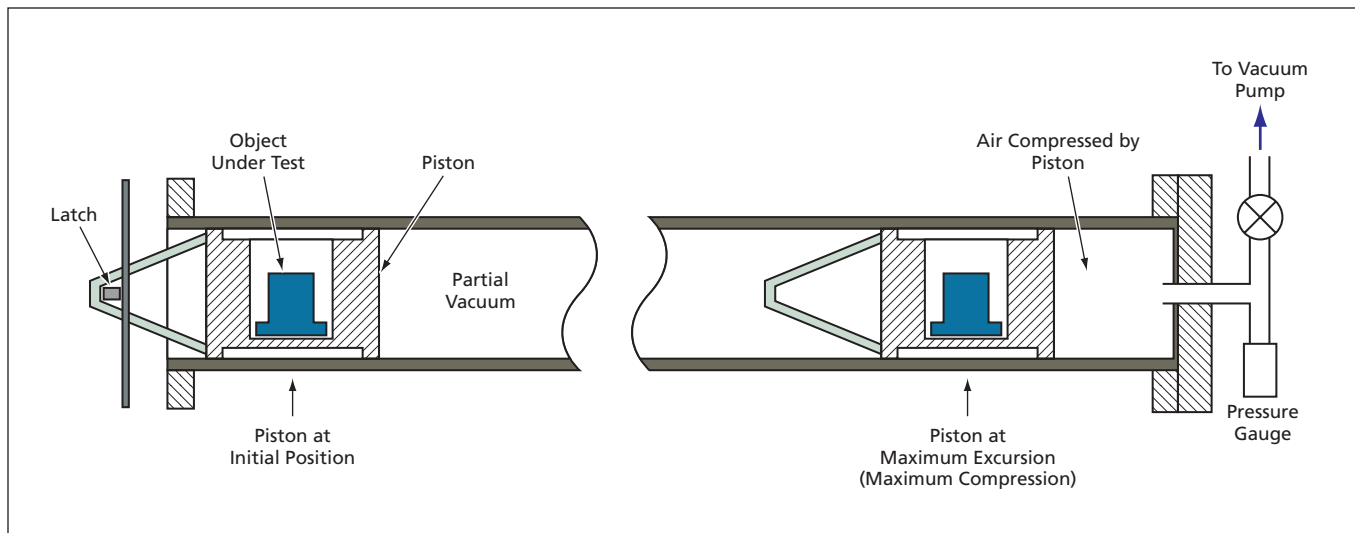
An apparatus has been designed and built for testing the effects, on moderate-sized objects, of cushioned decelerations having magnitudes ranging up to several hundred g [where g = normal Earth gravitational acceleration (≈ 9.8 m/s²)]. The apparatus was originally intended for use in assessing the ability of scientific instruments in spacecraft to withstand cushioned impacts of landings on remote planets. Although such landings can have impact velocities of

20 to 50 m/s, the decelerations must not exceed a few hundred g . This requires the deceleration to occur over a distance of as much as 50 cm in a time of tens of milliseconds. This combination of conditions is surprisingly difficult to simulate on the ground. The apparatus could also be used for general impact testing.

The apparatus is simple to build. Relative to drop-tower apparatuses that could produce equivalent impacts, this

apparatus is very compact. This apparatus is also relatively safe to operate because its design inherently prevents the object under test or any debris from accidentally striking persons or equipment in the vicinity.

The apparatus (see figure) includes a steel pipe having an inside diameter of 20 cm and a length of 216 cm. A lightweight polyethylene piston carries the object under test. The piston is sealed to the inner wall of the pipe by means of a



Atmospheric Pressure Drives the Piston along the partially evacuated pipe toward the closed end. The piston is then decelerated strongly when it compresses the remaining air at the closed end of the pipe.

gasket. One end of the pipe is open; the opposite end of the pipe is closed and connected to a vacuum pump.

At the beginning of a test, the piston is held at the open end of the pipe by use of a latch while the vacuum pump is activated to introduce a partial vacuum [typically, characterized by an absolute pressure of 0.2 bar (20 kPa)] between the piston and the closed end. Once the desired partial vacuum has been reached, the latch is released so that differential pressure (atmospheric minus partial vacuum) accelerates the piston along the pipe toward the closed end. The piston

reaches a maximum speed typically between 20 and 40 m/s, the exact value depending on the mass of the object under test and the starting pressure in the partly evacuated volume. As the piston approaches the closed end, it compresses the air ahead of it until, at a distance between 5 and 20 cm from the closed end, the pressure becomes high enough to stop the piston (and bounce it back toward its starting position). An accelerometer on the piston measures the impact deceleration.

The impact deceleration is a strong function of the amount of gas (and,

hence, of the pressure) initially in the partially evacuated volume at the closed end of the pipe. Therefore, it is easy to adjust the peak deceleration by adjusting the pressure of the partial vacuum. The maximum speed is not a strong function of the mass of the object under test or of the starting partial-vacuum pressure but can be tailored over a wide range by using pipes of different length.

This work was done by Pat R. Roach and Jeffrey Feller of Ames Research Center. Further information is contained in a TSP (see page 1). ARC-15085-1

Multi-Antenna Radar Systems for Doppler Rain Measurements

Use of multiple antennas would enable removal of platform Doppler contributions.

NASA's Jet Propulsion Laboratory, Pasadena, California

Use of multiple-antenna radar systems aboard moving high-altitude platforms has been proposed for measuring rainfall. The platforms contemplated in the proposal would be primarily spacecraft, but, in principle, the proposal could also apply to aircraft. The problem of measuring rainfall velocity from a moving platform is especially challenging because the velocity of the platform (especially in the case of a spacecraft) can be so large that it is difficult to distinguish between the rainfall and platform contributions to Doppler frequency shifts. Furthermore, nonuniform filling of radar beams can lead to biases in Doppler estimates. Although it might be possible to reduce these biases through improved data processing, a

potential alternative is to use multiple antennas positioned at suitable along-track intervals.

The basic principle of the proposed systems is a variant of that of along-track interferometric synthetic-aperture radar systems used previously to measure ocean waves and currents. The simplest system according to the proposal would include two antennas that would perform cross-track scans as in a prior rainfall-measuring radar system. The antennas would be located at different along-track positions. The along-track distance between them would be chosen, in conjunction with the along-track velocity of the platform and the radar pulse-repetition frequency (PRF), such that this distance would

equal the distance traveled by the platform between two successive pulses. (If necessary, the PRF could be adjusted to enforce this equality.) Thus, in effect, two sets of measurements would be performed at each platform position. Under this condition, extraction of the rainfall Doppler velocity without the platform contribution is substantially simplified and can be done with only minor modification of processing techniques traditionally used for ground-based Doppler radars.

This work was done by Stephen Durden, Simone Tanelli, and Paul Siqueira of Caltech for NASA's Jet Propulsion Laboratory. Further information is contained in a TSP (see page 1). NPO-44018

600-GHz Electronically Tunable Vector Measurement System

The design satisfies a complex set of technical and economic requirements.

NASA's Jet Propulsion Laboratory, Pasadena, California

A compact, high-dynamic-range, electronically tunable vector measurement system that operates in the frequency range from ≈ 560 to ≈ 635 GHz has been developed as a prototype of vector measurement systems that would be suitable for use in nearly-real-time active submillimeter-wave imaging. A judicious choice of intermediate frequencies makes it possible to utilize a significant amount of commercial off-the-shelf communication hardware in this system to keep its cost relatively low. The electronic tunability of this system has been proposed to be utilized in a yet-to-be-developed imaging system in which a frequency-dispersive lens would be used to steer transmitted and received beams in one dimension as a function of frequency. Then acquisition of a complete image could be effected by a combination of frequency sweeping for scanning in the aforesaid dimension and mechanical scanning in the perpendicular dimension.

As used here, "vector measurement system" signifies an instrumentation system that applies a radio-frequency (RF) excitation to an object of interest and measures the resulting amplitude and phase response, relative to either the applied excitatory signal or another reference signal related in a known way to applied excitatory signal. In the case of active submillimeter-wave imaging, the RF excitation would be a submillimeter-wavelength signal radiated from an antenna aimed at an object of interest, and the response signal would be a replica of

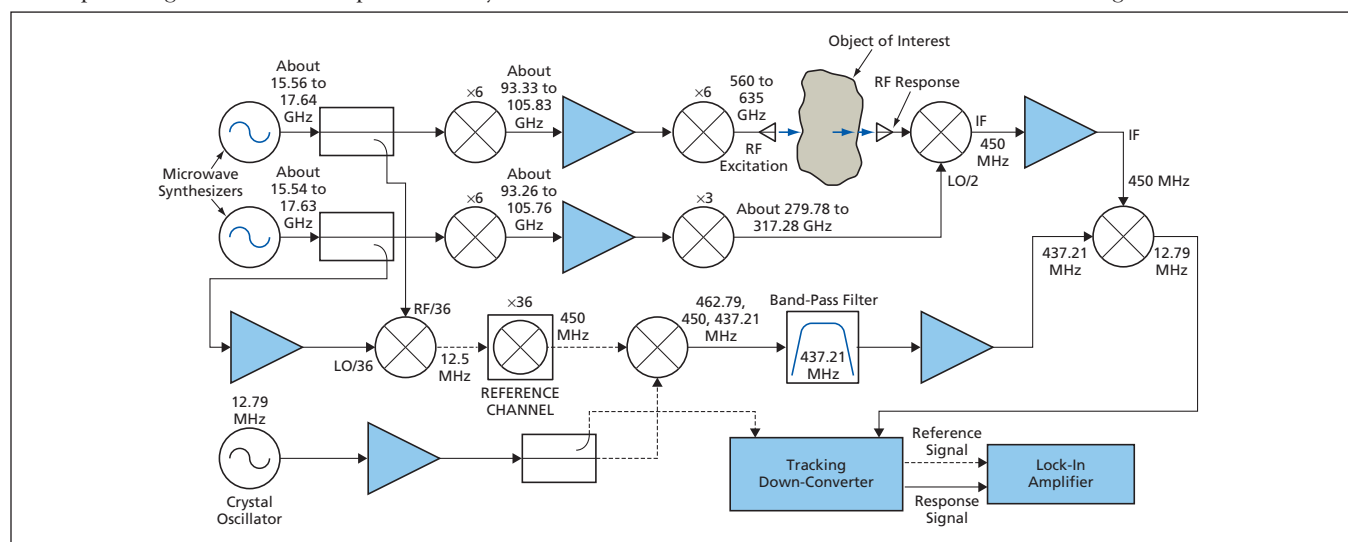
the RF excitation as modified in amplitude and phase by reflection from or transmission through the object.

The system is depicted schematically in the figure. The ultimate sources of the RF excitation and reference signals and of local-oscillator (LO) signals for use in down-conversion of the response signal are two compact, inexpensive microwave synthesizers that are electronically tunable over the frequency range from 14 to 18 GHz in increments of 250 kHz. The outputs of both synthesizers are multiplied $\times 6$ in frequency. The resulting signals, having frequencies in the neighborhood of 100 GHz, are amplified ≈ 20 dB by a pair of monolithic microwave integrated-circuit (MMIC) amplifiers. Then one of the amplified signals is further multiplied $\times 6$ in frequency for use as the RF excitation signal, while the other is further multiplied $\times 3$ in frequency for use as the LO signal in a subharmonically pumped mixer.

The RF excitation signal is radiated and made to pass through or reflect from an object of interest, and the response signal is mixed with the aforementioned subharmonic LO signal to generate a down-converted signal [denoted an intermediate-frequency (IF) signal in the radio art]. The RF and LO synthesizers are controlled from a laptop computer, which adjusts their frequencies to keep the IF constant at 450 MHz. Thus, the RF- and LO-synthesizer outputs differ in frequency by $450/36 = 12.5$ MHz.

The phase and amplitude measurements are performed indirectly, on signals derived from the IF signal, rather than directly on the RF response signal. For the purpose of generating a phase reference signal, portions of the outputs of the RF and LO synthesizers are mixed, yielding a 12.5-MHz signal, which is then multiplied $\times 36$ in frequency to obtain another 450-MHz signal. This 450-MHz signal cannot be used directly as the phase reference signal because the outputs of the inexpensive microwave synthesizers have such poor phase-noise characteristics that this signal and the 450-MHz IF signal are indistinguishable from the accompanying phase noise. Therefore, it is necessary to perform further processing as described next.

In particular, it is necessary to further reference both the 450-MHz IF and the 450-MHz reference signal to a stable source before detection. This involves down-converting the raw 450-MHz reference signal by 12.79 MHz by use of a 12.79-MHz fundamental crystal oscillator, a mixer, and a band-pass filter. The resultant 437.21-MHz signal is then mixed with the 450-MHz IF signal. Inasmuch as the phase noises of the 437.21-MHz signal and the 450-MHz IF signal are totally correlated, mixing these two signals cancels out that noise, leaving a 12.79-MHz signal that has the same amplitude and phase characteristics (minus the synthesizer noise) as does the 450-MHz IF signal.



This **Vector Measurement System** is made from a combination of commercially available and custom components. The complexity of the reference channel is necessitated by a requirement to cancel phase noise that originates in the microwave synthesizers.

It should be noted that any 450-MHz signal passing through the 437.21-MHz band-pass filter would be down-converted along with the 437.21-MHz signal, resulting in cross-talk and loss of dynamic range. It is therefore essential that the 437.21-MHz band-pass filter have extremely high rejection at 450 MHz.

The 12.79-MHz signals in the response and reference channels are converted to a frequency of ≈ 66 kHz in a tracking down-converter, then detected by a lock-in amplifier that functions as a variable-bandwidth magnitude and

phase receiver. The bandwidth and gain are controlled by a laptop computer. The vector DC outputs of the lock-in amplifier are read by an analog data-acquisition card in the computer, wherein these readings are converted to polar format. At maximum detection bandwidth, real-time acquisition speeds of $>3,000$ points per second are possible.

This work was done by Robert Dengler, Frank Maiwald, and Peter Siegel of Caltech for NASA's Jet Propulsion Laboratory. Further information is contained in a TSP (see page 1).

In accordance with Public Law 96-517, the contractor has elected to retain title to this invention. Inquiries concerning rights for its commercial use should be addressed to:

*Innovative Technology Assets Management
JPL*

*Mail Stop 202-233
4800 Oak Grove Drive
Pasadena, CA 91109-8099
(818) 354-2240*

E-mail: iaoffice@jpl.nasa.gov

Refer to NPO-43394, volume and number of this NASA Tech Briefs issue, and the page number.

Modular Architecture for the Measurement of Space Radiation

New architecture developed with improved capabilities adds radiation hardness.

Lyndon B. Johnson Space Center, Houston, Texas

A modular architecture has been conceived for the design of radiation-monitoring instruments used aboard spacecraft and in planetary-exploration settings. This architecture reflects lessons learned from experience with prior radiation-monitoring instruments. A prototype instrument that embodies the architecture has been developed as part of the Mars Advanced Radiation Acquisition (MARA) project. The architecture is also applicable on Earth for radiation-monitoring instruments in research of energetic electrically charged particles and instruments monitoring radiation for purposes of safety, military defense, and detection of hidden nuclear devices and materials.

Whereas prior such instruments have contained non-radiation-hardened parts, an instrument according to this architecture is made of radiation-hardened/radiation-tolerant parts, enabling the instrument to resist damage by the radiation that it is intended to measure. One of the building blocks in this modular architecture is a single-channel radiation-detection circuit, which is essentially a detector interface, signal-processing and measurement circuit, dedicated to a single radiation detector that provides radiation-event data to the CPU. The interface between the single-channel radiation-detection circuit and the rest of the instrument is a PC/104 computer-bus interface. [PC/104 is an industry standard for compact, stackable modules that are compatible (in architecture, hardware, and software) with personal-computer data and power-bus circuitry.] Multiple single-channel radiation-detection cir-

cuits can be stacked to create a multiple-detector instrument.

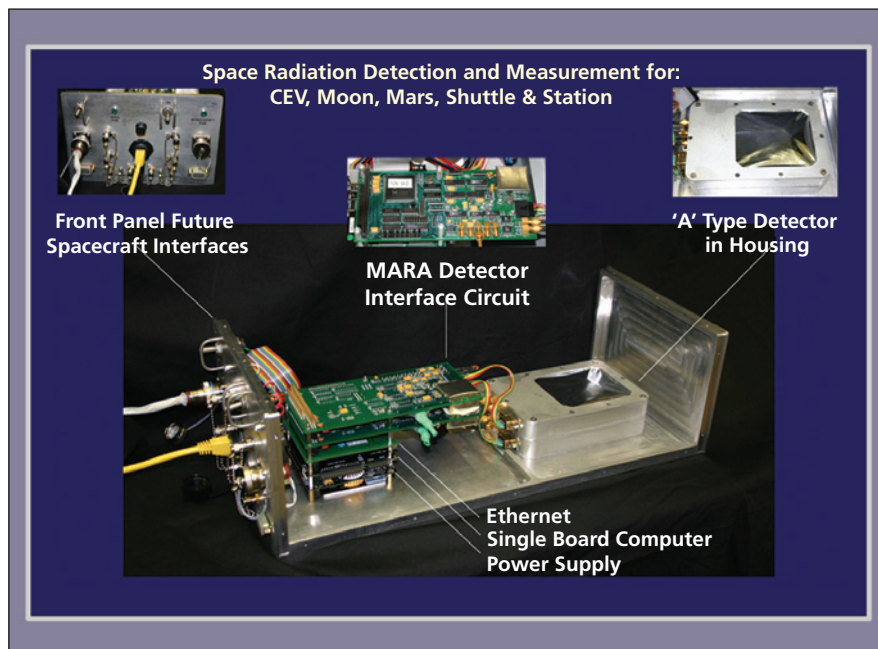
The present architecture as embodied in the MARA instrument design offers the following advantages over the architectures and designs of prior radiation-monitoring systems:

The detector interface circuitry in prior instruments included voltage-feedback operational amplifiers, which do not enable accurate tracking of the rising edges of incoming pulses and, as a result, do not enable deterministic discrimination among different levels of radiation events. In contrast, the MARA circuit design provides the capa-

bility to more accurately differentiate among different types of energetic charged particles.

Unlike prior designs, the MARA design provides for correlated double sampling, which offers the advantage of subtraction of correlated noise between reset samples and data samples, thereby reducing spurious offsets and the effects of low-frequency noise.

Prior designs do not afford enough dynamic range to enable detection of both low- and high-energy events without adjustment by an operator. The MARA design features 16-bit quantization depth, which provides sufficient dynamic range to en-



MARA Instrument Phase I Prototype is shown in two-detector configuration. (Note: CEV is Crewed Exploration Vehicle.)

able detection of both low- and high-energy events using the same circuit configuration.

The event-detection circuits of prior instruments do not employ hysteresis and, as a result, spurious trigger signals are generated during the rising and falling edges of pulses being detected. The use of hysteresis in the MARA design ensures that only one pulse is produced for each rising edge and for each radiation event.

Prior designs do not employ distributed processing: Instead, they rely on central computers or processors to poll, sample, and store data from multiple boards in the instruments. In contrast, the present architecture provides for distributed processing with local memory, enabling each board to independently sample events and store data pertaining to them. This architecture facilitates prompt reading of time-critical data signals in a consistent operation. Distributed processing with local memory also allows identification of coincident detec-

tions by multiple radiation-detection boards through comparison of time stamps attached to data collected by individual boards.

Prior designs employ custom bus interfaces rather than industry-standard ones. Adherence to the PC/104 bus-interface standard in the present architecture (1) makes the architecture more amenable to diverse applications, (2) facilitates customization and reconfiguration of a suite of radiation detectors through stacking of multiple circuit boards, (3) enables incorporation of other interface hardware that also adhere to the PC/104 standard (this saves costs, time and risk), and (4) enables inclusion or exclusion of various communication interfaces through addition or removal of circuit cards of different types.

Prior designs do not provide for in-system reprogrammability of radiation-detection firmware. The MARA design enables remote loading of modifications of firmware and/or replacement of cor-

rupted firmware files with firmware files of known integrity.

Prior designs used a text-based user interface for command and control. MARA employs an easy-to-use graphical user interface, with point-and-click functionality. The control console application also provides several real-time displays, when in the ground mode. Data received from MARA is displayed as detector pulse height spectrum graph, coincident data x - y scatter plot, and historical event count tracking. These displays enable rapid system configuration and calibration.

This work was done by Paul Delaune, Kathryn Turner, and S. Douglas Holland of Johnson Space Center; William R. Carson of Muniz Engineering; and Fadi Riman of Lockheed Martin.

Inquiries concerning rights for the commercial use of this invention should be addressed to the Technology Transfer Office, Johnson Space Center, (281) 483-3089. Refer to MSC-24042/38/41/228.



VLSI Design of a Turbo Decoder

The design is readily adaptable to diverse applications.

NASA's Jet Propulsion Laboratory, Pasadena, California

A very-large-scale-integrated-circuit (VLSI) turbo decoder has been designed to serve as a compact, high-throughput, low-power, lightweight decoder core of a receiver in a data-communication system. In a typical contemplated application, such a decoder core would be part of a single integrated circuit that would include the rest of the receiver circuitry and possibly some or all of the transmitter circuitry, all designed and fabricated together according to an advanced communication-system-on-a-chip design concept.

Turbo codes are forward-error-correction (FEC) codes. Relative to older FEC codes, turbo codes enable communication at lower signal-to-noise ratios and offer greater coding gain (closer to the Shannon theoretical limit). In addition, turbo codes can be implemented by relatively simple hardware. Therefore, turbo codes have been adopted as standard for some advanced broadband communication systems.

In general, a turbo encoder is equivalent to two convolutional encoders plus a lookup table that stores interleaver addresses; a turbo decoder (see figure) includes a channel metric and parsing block, two soft-input/soft-output (SISO) decoders (denoted SISO1 and SISO2), and a random-access memory (RAM) for interleaving/deinterleaving functions.

The received signal is first processed and parsed through the channel metric and parsing block, the output of which is a sequence of estimates that indicate how closely each received bit is deemed to resemble a one or a zero. On the basis of these estimates, SISO1 makes "soft" decisions: a soft decision is a statement of the probability that each received bit is a one or a zero, based on the preceding sequence of bits.

The soft decisions made by SISO1 are interleaved to be included in the input to SISO2, which then makes soft decisions based on both the estimates from the channel metric and parsing block and the soft decisions from SISO1. These soft decisions are again interleaved and sent as input to SISO1. Now, SISO1 has more information to use than it had on the previous iteration and it strives to use the additional information to make a more accurate decision. The iterative decoding process is repeated either a fixed number of times or until some other criterion is satisfied. Then hard decisions are made on the basis of the soft decisions. Intuitively, if the probability of a zero exceeds that of a one for a given bit, then the hard decision will be that a zero was transmitted.

A description of the practical implementation of the above-described decoder architecture in terms of functional

blocks of circuitry, the functions (including memory reading and writing, calculations, and comparisons) performed by the blocks, and timing of the functions would greatly exceed the space available for this article. It must suffice to summarize by reporting that some details of the architecture of the implementation are especially important for the overall design: The details in question include those of the timing of memory reading and writing operations, a finite state machine in each SISO decoder, a module in each SISO decoder that performs forward and backward calculations, a module in each SISO decoder that performs the soft-output calculations, and the interleaver/deinterleaver module.

Overall, the design of the decoder is parameterizable: that is, by adjusting the parameters of an otherwise generic design, one can modify the design to fit into such communication-on-a-system products as transceivers in satellite communication systems, transceivers in wireless local-area networks, digital television receivers, cable modems, digital video broadcast receivers, and digital subscriber lines. A prototype of the decoder has been implemented in a field-programmable gate array (FPGA) chip that performs forward error correction on data streaming at a rate of 15 Mb/s while consuming a power of only 0.1 W.

This work was done by Wai-Chi Fang of Caltech for NASA's Jet Propulsion Laboratory. Further information is contained in a TSP (see page 1).

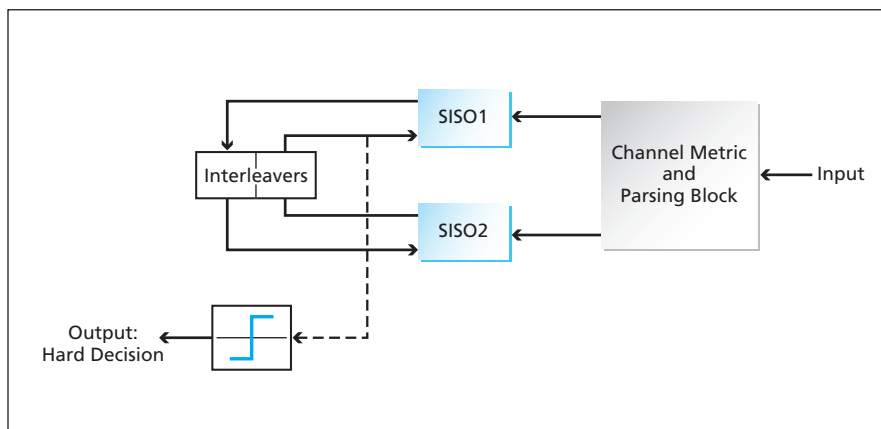
In accordance with Public Law 96-517, the contractor has elected to retain title to this invention. Inquiries concerning rights for its commercial use should be addressed to:

*Innovative Technology Assets Management
JPL*

*Mail Stop 202-233
4800 Oak Grove Drive
Pasadena, CA 91109-8099
(818) 354-2240*

E-mail: iaoffice@jpl.nasa.gov

Refer to NPO-40392, volume and number of this NASA Tech Briefs issue, and the page number.



A **Turbo Decoder** engages in an iterative process in which incoming data are considered along with prior soft decisions in an effort to reach more accurate hard decisions concerning received bits. A parameterizable design for a practical decoder has been implemented in an FPGA.



Architecture of an Autonomous Radio Receiver

The receiver would configure itself to receive an initially unknown signal.

NASA's Jet Propulsion Laboratory, Pasadena, California

A program to develop an autonomous radio receiver compatible with a variety of digital communication schemes is underway. The proposed receiver, to be implemented largely in software, would configure itself to receive an incoming signal without much *a priori* knowledge of defining characteristics of the signal. These characteristics include the carrier frequency and phase, modulation type, modulation index, symbol timing, data rate, type of code, and signal-to-noise ratio.

Heretofore, radio receivers have been configured manually, on the basis of prior knowledge of the signals to be received. In situations in which prior knowledge of signal types is not available and/or it is necessary to receive signals of different types at different times, manual re-configuration can be impractical and excessively time-consuming. Such situations can be expected to arise increasingly frequently in spacecraft communications, military interception of signals transmitted by adversaries, and cellular telephony.

The proposed receiver would include estimating and classifying modules that would analyze the incoming signal to determine its defining characteristics and would then configure itself on the basis of the outputs of these modules. It is assumed that a signal to be received would arrive through a single channel, would be amplitude (pulse)- and/or phase-modulated, and may or may not include a residual carrier. Each of the estimating and classifying modules would be capable of recognizing one of the defining characteristics of such a signal.

The quality of the output of each module would be limited to the extent to which that module lacked knowledge of the outputs of the other modules. For example, it would not be feasible to classify the modulation type prior to classifying the data rate and obtaining the symbol timing. If one were to use conventional estimation and tracking designs, one would quickly encounter a "chicken and egg" problem: nearly every estimating module would

need the outputs of the other estimating modules before the receiver could make a maximum-likelihood estimate. The architecture of the proposed receiver would solve this problem by defining the order in which the modules could be operated, at least suboptimally, during the

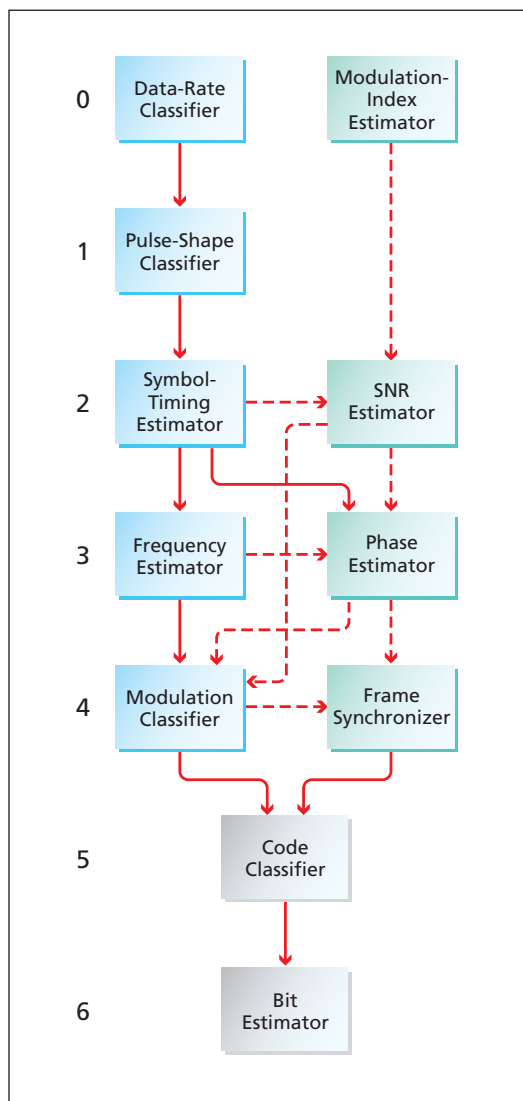
levels for which processing at some level, i , must be performed before processing at level $i + 1$.

The dashed arrows in the figure indicate additional dependencies that are not strictly required but could, if utilized, result in improved performance (possibly at the cost of increased latency). For example, the modulation classifier could operate noncoherently, without input from the phase-tracking loop, but if it waited for that input, its performance would be improved. This arrangement would implement a workable "boot-strapping" approach to estimating and classifying all of the parameters necessary for the proper operation of the entire receiver.

Initially, no module at a given level could make use of any signal attribute estimated at a level beneath it. This limitation would significantly adversely affect performance, and is inherent in any non-iterative autonomous signal-parameter-estimation algorithm. A fundamental innovation in the proposed receiver, intended to partly overcome this limitation, would be an iterative message-passing architecture: After each module completed its first estimate or classification in the proper boot-strap order, lower-level modules would send soft information to higher-level modules. In a second iteration, each module would make use of the soft information to improve its performance. After several iterations, the message-passing system would reach a reasonable convergence. It has been shown that systems like this one are typically quite robust, and can provide near-maximum-likelihood joint estimation and decoding performance.

This work was done by Jon Hamkins, Marvin Simon, Dariush Divsalar, and Samuel Dolinar of Caltech for NASA's Jet Propulsion Laboratory. Further information is contained in a TSP (see page 1).

This invention is owned by NASA, and a patent application has been filed. Inquiries concerning nonexclusive or exclusive license for its commercial development should be addressed to the Patent Counsel, NASA Management Office-JPL. Refer to NPO-41446.



Estimating and Classifying Modules of the proposed autonomous receiver would operate in the order of dependency represented by this diagram.

first iteration of estimation. This order is depicted in the figure, wherein solid arrows indicate a strict dependency, meaning that the module at the head of an arrow cannot proceed without input in the form of the output of the module at the tail of the arrow. The modules would be arranged in the minimum number of

Improved On-Chip Measurement of Delay in an FPGA or ASIC

Input and output buffers and the associated delays are eliminated.

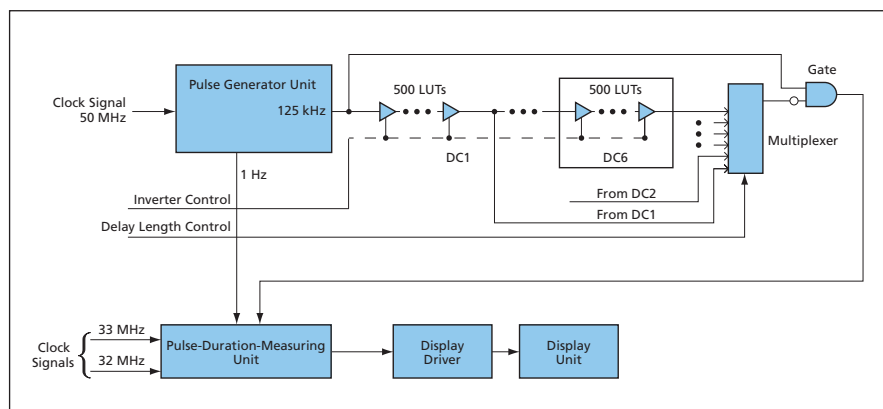
NASA's Jet Propulsion Laboratory, Pasadena, California

An improved design has been devised for on-chip-circuitry for measuring the delay through a chain of combinational logic elements in a field-programmable gate array (FPGA) or application-specific integrated circuit (ASIC). Heretofore, it has been the usual practice to use either of two other types of on-chip delay-measuring circuits:

- A delay chain of inverters is incorporated into the FPGA or ASIC chip along with an input port for feeding the inverter chain and an output port for feeding a signal to off-chip measurement circuitry. The disadvantage of this design is that the measurement is inaccurate because it includes delays in buffers that are parts of the input and output ports.
- The delay chain is arranged as a ring oscillator. The disadvantage of this design is that the delay chain does not always oscillate as expected.

The improved design overcomes the disadvantages of both older designs. In the improved design, the delay chain does not include input and output buffers and is not configured as an oscillator. Instead, the delay chain is made part of the signal chain of an on-chip pulse generator. The duration of the pulse is measured on-chip and taken to equal the delay.

In this design (see figure) the delay chain comprises six sub-chains denoted DC1 through DC6. Each sub-chain contains 500 lookup tables (LUTs), which are used as universal logic gates that implement the combinational logic in the FPGA or ASIC. The LUTs are programmed to act as either inverters or buffers, depending on the position of a switch on an external circuit board. The output end of each sub-chain except the last one is connected to the input end of the next sub-chain; the output end of



The **Delay Chain** is part of an on-chip instrumentation system that generates pulses and measures their duration. Control and clock signals are generated by external circuitry.

each subchain is also connected to one of six input terminals of a multiplexer. By setting of switches in the multiplexer controlled by external circuitry, the length of the delay chain can be set to any value between 500 and 3,000 LUTs in increments of 500 LUTs.

Also on the external board are two crystal-controlled oscillators. One oscillator generates a clock signal at a nominal frequency of 50 MHz; the other generates a clock signal, at a nominal frequency of 33 MHz, which is not synchronized with the 50-MHz signal. The 50-MHz signal is used for the majority of the FPGA logic. The 33-MHz signal is fed to an on-chip pulse-duration-measuring unit.

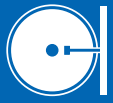
The on-chip delay-measuring circuitry includes a pulse-generator unit, wherein the 50-MHz signal is divided in frequency to generate two outputs: (1) a 1-pulse-per-second clock signal that is fed to the on-chip pulse-duration-measuring unit and (2) a train of pulses, at frequency of 125 kHz, that is fed as input to the delay chain.

A gate that follows the multiplexer accepts inputs from both ends of the delay

chain. In response, the gate generates a 125-kHz train of pulses, the duration of which equals the delay. This pulse train is fed to the pulse-duration-measuring unit. The duration of the pulses in this train is what is measured. The complexity of the pulse-duration-measurement process is such that a complete description is not possible within the space available for this article. It must suffice to summarize by saying that the process involves a combination of sampling the 125-kHz pulses by use of the 33-MHz clock signals during a fixed period of 1 second, counting the numbers of sampling periods during which the pulses are on, then averaging and displaying the result.

This work was done by Yuan Chen, Gary Burke, and Douglas Sheldon of Caltech for NASA's Jet Propulsion Laboratory. Further information is contained in a TSP (see page 1).

This invention is owned by NASA, and a patent application has been filed. Inquiries concerning nonexclusive or exclusive license for its commercial development should be addressed to the Patent Counsel, NASA Management Office-JPL. Refer to NPO-43348.



Resource Selection and Ranking

Surfer is an extensible framework for selecting and ranking grid resources. A resource is defined as anything that needs selecting such as compute resources, storage resources, and data resources. The user specifies the set of resource types desired, the constraints that must hold over all the resources, and the ranking function to be used to order the resources. For each request received, Surfer returns a set of resource tuples, where each tuple contains a resource instance for each resource type requested, each tuple satisfies the specified constraints, and tuples are ordered by descending values of the given ranking function. Constraints and ranking functions are Boolean and numeric expressions, respectively, using a set of built-in arithmetic, Boolean and relational operators, and a set of functions supplied by information providers, which are implemented independently of the framework and integrated into the system using a single configuration line.

Providers supply functions of arbitrary type that represent selected information such as the number of CPUs of a compute resource, free disk space of a storage resource, etc. Providers also supply queries used to generate resource sets that define the set of resources that are selectable. Information providers are invisible to the end user, who only sees the set of resource types selectable as well as the set of functions available. The frame-

work decides which provider is responsible for each function, whether to use queries or function calls, and how results are correlated.

This program was written by Paul Kolano of Advanced Management Technology for Ames Research Center. Further information is contained in a TSP (see page 1).

Accident/Mishap Investigation System

InvestigationOrganizer (IO) is a Web-based collaborative information system that integrates the generic functionality of a database, a document repository, a semantic hypermedia browser, and a rule-based inference system with specialized modeling and visualization functionality to support accident/mishap investigation teams. This accessible, online structure is designed to support investigators by allowing them to make explicit, shared, and meaningful links among evidence, causal models, findings, and recommendations.

The semantic hypermedia component includes a customizable ontology that specifies various types of items such as people, places, events, causes, systems, and associated information products relevant to mishap investigations. The ontology also describes the important properties of each item, and details the potential relationships among items. Items stored in the repository are classified according to the ontology. Users can set properties for stored items, and

can associate a relevant electronic file with each one. Links between items can be established based on the relationships defined in the ontology, making the items viewable with the hypermedia browser to navigate the established links of interrelated items.

In addition to providing repository functionality, users can create and view overarching analysis models that specify causal factors, or hypothesized event sequences, leading up to the mishap. The causal models are linked to repository items that provide evidence to support or refute the hypothesized causes. The models can be viewed with linear, hierarchical, or network diagrams displayed by the user interface. The IO system was sponsored by the Engineering for Complex Systems program to address systemic challenges in NASA. It was built as a customized application of the SemanticOrganizer hypermedia system, and has been used in investigations ranging from small property damage cases to the loss of the space shuttle *Columbia*.

This program was developed by Richard Keller, Shawn Wolfe, Yuri Gawdiak, Robert Carvalho, Tina Panontin, and James Williams of Ames Research Center, and Ian Sturken of QSS Group, Inc. Further information is contained in a TSP (see page 1).

This invention is owned by NASA and a patent application has been filed. Inquiries concerning rights for the commercial use of this invention should be addressed to the Ames Technology Partnerships Division at (650) 604-2954. Refer to ARC-15073-1.



Simplified Identification of mRNA or DNA in Whole Cells

This test can be performed using compact, low-power equipment.

Ames Research Center, Moffett Field, California

A recently invented method of detecting a selected messenger ribonucleic acid (mRNA) or deoxyribonucleic acid (DNA) sequence offers two important advantages over prior such methods: it is simpler and can be implemented by means of compact equipment. The simplification and miniaturization achieved by this invention are such that this method is suitable for use outside laboratories, in field settings in which space and power supplies may be limited.

This method is related to the methods described in "Simplified Microarray Technique for Identifying mRNA in Rare Samples" (ARC-15177-1), *NASA Tech Briefs*, Vol. 31, No. 1 (January 2007), page 60. Like the methods described in the cited prior article as well as older, more complex methods, the present method is based partly on hybridization of nucleic acid, which is a powerful technique for detection of specific complementary nucleic acid sequences and is increasingly being used for detection of changes in gene expression in microarrays containing thousands of gene probes. Like one of the methods described in the cited prior article, the present method provides for identification of mRNA or DNA from whole cells.

In the present method, one begins by preparing one or more reference substance(s) and a reference slide that contains one or more compartment(s) —

one compartment for each reference substance. Each reference substance includes a selected mRNA or DNA sequence labeled with horseradish peroxidase. [Preferably, the mRNA or DNA is prepared by polymerase chain reaction (PCR) amplification.] Each reference substance is formulated to be solid at a low storage temperature (about 4 °C) and to become liquid at a higher temperature (no more than about 42 °C). Each reference substance is placed in its assigned compartment on the slide, then the slide is stored under refrigeration until it is used.

One also prepares a plate containing one or more microwell(s). If there is more than one microwell, then the microwells are arrayed in a pattern to register with the compartments containing the reference substances on the slide. Cells to be tested for the selected mRNA or DNA sequence(s) [more specifically, cells that contain substances that may or may not include the selected mRNA or DNA sequence(s)] are prepared by making holes in their membranes large enough to enable molecules of the reference substances to enter. One or more of the cells is placed in each microwell.

At testing time, the reference slide is removed from cold storage and placed in contact with the microwell plate, positioned so that the compartments containing the reference substances are reg-

istered with the microwells containing the cells. The plate-and-slide assembly is then warmed to liquefy the reference substances so that they flow into the microwells and through the holes into the cells. The reference substance reacts with substances in the cells, and the products of these reactions are then hybridized. If a cell contains a target substance (a substance that includes the selected mRNA or DNA), then the reference and target substances react to form reference-sequence/target-substance conjugate molecules. The reaction products are treated with a chemiluminescence solution, then illuminated with light in a selected wavelength interval and subjected to a chemiluminescence scan. The presence or a sense of the reference-sequence/target-substance conjugate molecules (and, hence, the presence or absence of the selected mRNA or DNA in the cells) is indicated by the presence or absence of corresponding chemiluminescence spots in the scan image.

This work was done by Eduardo Almeida of Ames Research Center and Geeta Kadambi of National Space Grant Foundation.

This invention is owned by NASA, and a patent application has been filed. Inquiries concerning rights for the commercial use of this invention should be addressed to the Ames Technology Partnerships Division at (650) 604-2954. Refer to ARC-15448-1.

Printed Multi-Turn Loop Antennas for RF Biotelemetry

Compact antennas afford hemispherical coverage at any linear polarization.

John H. Glenn Research Center, Cleveland, Ohio

Printed multi-turn loop antennas have been designed for contactless powering of, and reception of radio signals transmitted by, surgically implantable biotelemetric sensor units operating at frequencies in the vicinity of 300 MHz. In the original intended application of these antennas, the sensor units would

be microelectromechanical systems (MEMS)-based devices now being developed for monitoring physiological parameters of humans during space flights. However, these antennas and the sensor units could just as well be used for physiological monitoring on Earth.

Figure 1 depicts one such antenna, consisting of a thin metal strip laid out in a multi-loop pattern on a dielectric substrate. Other components are also mounted on the dielectric substrate. For maximum sensitivity in reception, a Pi network (which comprises lumped-element inductors and capacitors) is used to

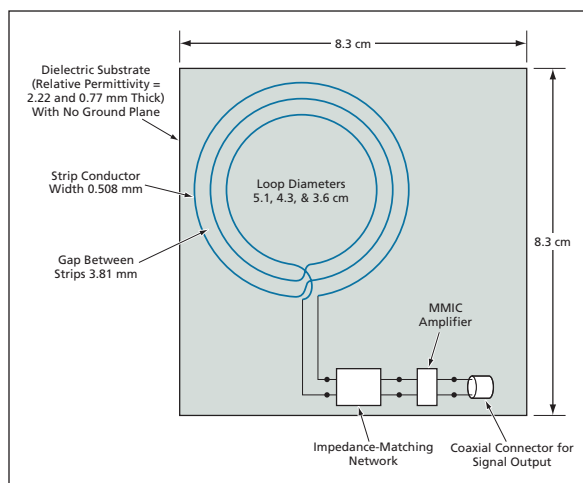


Figure 1. A Multi-Turn Loop Antenna on a dielectric substrate is small enough to be part of a hand-held telemetry-reception unit.

match impedances between the antenna terminals and the input terminals of a monolithic microwave integrated circuit (MMIC) low-noise amplifier. The output

processing circuits could be mounted in the central regions of the loops.

In a typical medical diagnostic situation, the signal radiated by an im-

of the amplifier is sent to other circuits through a coaxial cable. The antenna and the other components and circuits mentioned above are all parts of a hand-held telemetry-reception unit.

In comparison with prior spiral, disk-coil, and solenoid-coil antennas that have been considered for use in receiving telemetry from implantable sensors, the antennas of the present type are smaller. In addition, the present antennas offer potential for further miniaturization in that, in principle, signal-

planted sensor could have vertical, horizontal, or slanted polarization. Hence, to emulate all possibilities, the radiation pattern of a loop antenna of the present type was measured in reception of a signal transmitted by a dipole antenna in vertical, horizontal, and slanted (45°) orientations. The results of these measurements (see Figure 2) show that the antenna provides hemispheric coverage and is capable of receiving signals under the aforementioned linear-polarization conditions.

This work was done by Rainee N. Simons, David G. Hall, and Félix A. Miranda of Glenn Research Center. Further information is contained in a TSP (see page 1).

Inquiries concerning rights for the commercial use of this invention should be addressed to NASA Glenn Research Center, Innovative Partnerships Office, Attn: Steve Fedor, Mail Stop 4-8, 21000 Brookpark Road, Cleveland, Ohio 44135. Refer to LEW-17879-1.



Making Ternary Quantum Dots From Single-Source Precursors

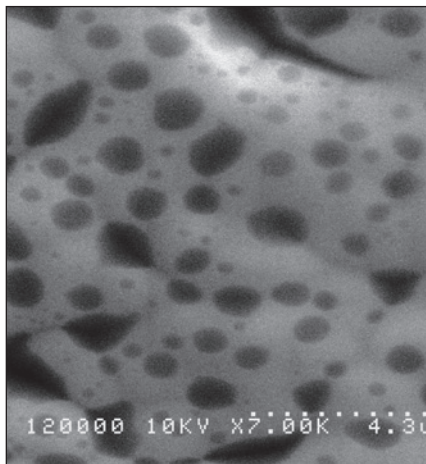
Relative to a prior process, this process is simpler and safer.

John H. Glenn Research Center, Cleveland, Ohio

A process has been devised for making ternary (specifically, CuInS_2) nanocrystals for use as quantum dots (QDs) in a contemplated next generation of high-efficiency solar photovoltaic cells. The process parameters can be chosen to tailor the sizes (and, thus, the absorption and emission spectra) of the QDs.

The process used heretofore to synthesize quantum dots in general involves *in situ* pyrolysis of reagents in the presence of a passivating solvent/ligand that not only serves as a medium for the formation of the QDs via pyrolysis, but also readily coordinates to the surfaces of the QDs, thereby preventing further nucleation. The prevention of further nucleation, also known as capping, serves to regulate the size of the QDs.

The present process is simpler and involves less handling of toxic reagents. Instead of the reagents of the prior process, one uses a compound of the type described in the first of the two immediately preceding articles, "Improved Single-Source Precursors for Solar-Cell Abs-



CuInS_2 Nanocrystals and Agglomerates on a polished silicon surface are shown in this scanning electron micrograph. The average diameter of the nanocrystals in this batch is 13.4 nm.

sorbers." The single-source precursor is dissolved in trioctylphosphine under an inert atmosphere. The resulting solution is subsequently injected into a hot stirred so-

lution of trioctylphosphine oxide (TOPO) in order to facilitate controlled decomposition of the precursor to obtain the desired capped ternary quantum dots.

Aliquots of the solution are removed during the formation of the nanocrystals and are monitored via ultraviolet/visible-light spectroscopy to obtain information on the sizes of the nanocrystals. When the desired size range is reached, the reaction solution is cooled and methanol is added to remove excess precursor, leaving the TOPO-capped ternary nanocrystals to be harvested. The figure shows the product of one of several experiments performed to test this process.

This work was done by Sheila Bailey, Kulbinder Banger, Stephanie Castro, and Aloysius Hepp of Glenn Research Center. Further information is contained in a TSP (see page 1).

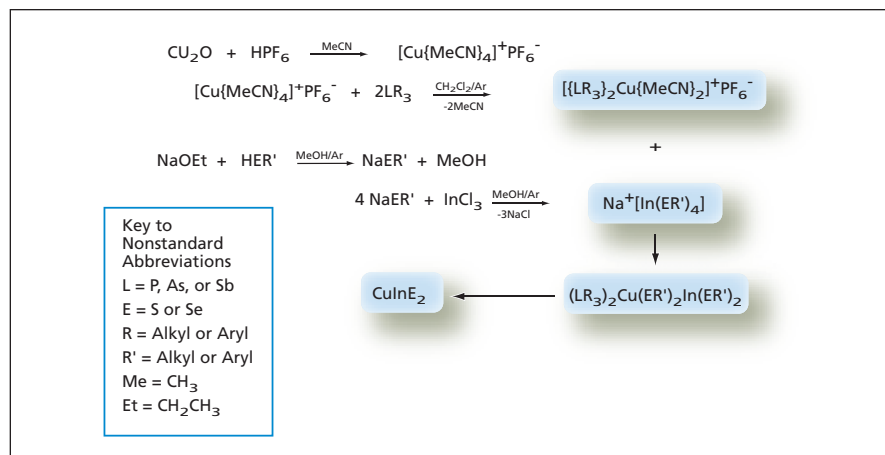
Inquiries concerning rights for the commercial use of this invention should be addressed to NASA Glenn Research Center, Innovative Partnerships Office, Attn: Steve Fedor, Mail Stop 4-8, 21000 Brookpark Road, Cleveland, Ohio 44135. Refer to LEW-17446-1.

Improved Single-Source Precursors for Solar-Cell Absorbers

Deposition properties and final compositions can be tailored.

John H. Glenn Research Center, Cleveland, Ohio

Improved single-source precursor compounds have been invented for use in spray chemical vapor deposition (spray CVD) of chalcopyrite semiconductor absorber layers of thin-film solar photovoltaic cells. The semiconductors in question are denoted by the general formula $\text{CuIn}_x\text{Ga}_{1-x}\text{S}_y\text{Se}_{2-y}$, where $x \leq 1$ and $y \leq 2$. These semiconductors have been investigated intensively for use in solar cells because they exhibit long-term stability and a high degree of tolerance of radiation, and their bandgaps correlate well with the maximum photon power density in the solar spectrum. In addition, through selection of the proportions of Ga versus In and S versus Se, the bandgap of $\text{CuIn}_x\text{Ga}_{1-x}\text{S}_y\text{Se}_{2-y}$ can be tailored to a



These **Sequences of Chemical Reactions** are representative of the synthesis of a single-source precursor, in this case, $[\{[\text{LR}_3]_2\text{Cu}(\text{ER}')_2\text{In}(\text{ER}')_2\}]$ followed by formation of the chalcopyrite semiconductor (in this case, CuInE_2) from the precursor.

value between 1.0 and 2.4 eV, thus making it possible to fabricate cells containing high and/or graded bandgaps.

A "single-source precursor compound" is a single molecular compound that contains all the required elements, which when used under the spray CVD conditions, thermally decomposes to form $\text{CuIn}_x\text{Ga}_{1-x}\text{S}_y\text{Se}_{2-y}$. Relative to the use of multiple precursor reagents, the use of single-source precursors offers the advantage of better regulation of the chemical composition of the deposit, less susceptibility to contamination, and, most importantly, a simplified fabrication process.

The improved single-source precursor compounds of the invention are denoted by the general formula

$[(\text{LR}_3)_2\text{Cu}(\text{ER}')_2\text{M}(\text{ER}')_2]$, where L signifies P, As, or Sb; R or R' signifies an alkyl or aryl group; and E signifies S or Se. The general formula and molecular structure afford flexibility for tailoring the precursor to suit a specific CVD spray process and to tailor the chemical composition (more specifically, the proportions x and y) of $\text{CuIn}_x\text{Ga}_{1-x}\text{S}_y\text{Se}_{2-y}$ formed in the process. In addition, by choosing L, R, R', and E according to their steric and electronic properties, one can tailor decomposition temperatures and the phases in the deposit.

A single-source precursor of the invention can be synthesized by the reaction of a stabilized Cu(I) cation with an In(III) or Ga(III) chalcogenide anion prepared *in situ* by reaction of the conju-

gate acid of the thiol or selenol with NaOEt (where Et signifies an ethyl group) in CH_3OH , as in the example of the figure. Alternatively, one could synthesize a single-source precursor by use of commercially available reagents in a new facile one-pot process: For example one could react NaSCH_3 with InCl_3 and add CuCl and PR_3 .

This work was done by Kulbinder K. Banger, Jerry Harris, and Aloysius Hepp of Glenn Research Center. Further information is contained in a TSP (see page 1).

Inquiries concerning rights for the commercial use of this invention should be addressed to NASA Glenn Research Center, Innovative Partnerships Office, Attn: Steve Fedor, Mail Stop 4-8, 21000 Brookpark Road, Cleveland, Ohio 44135. Refer to LEW-17445-1.

Spray CVD for Making Solar-Cell Absorber Layers

Spray CVD combines the advantages of metalorganic CVD and spray pyrolysis.

John H. Glenn Research Center, Cleveland, Ohio

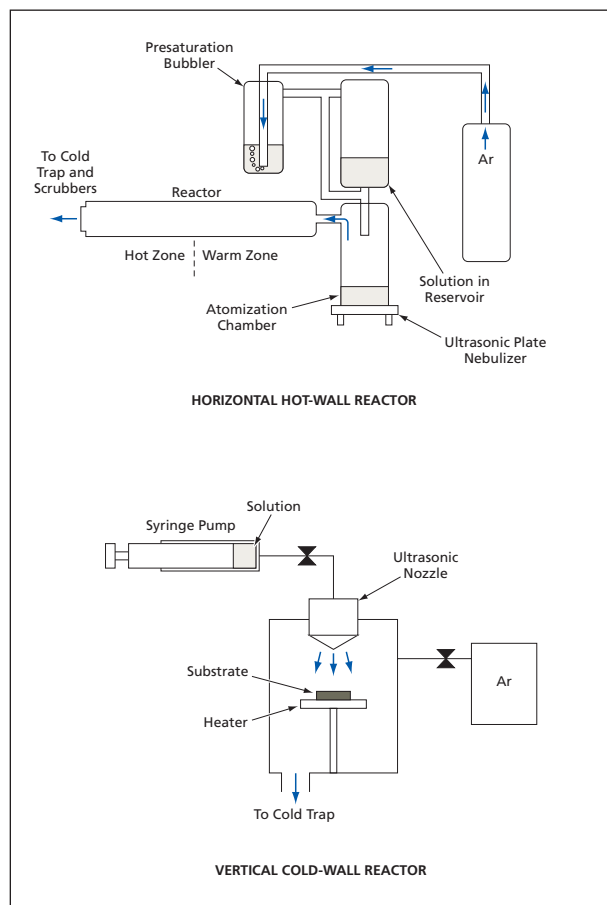
Spray chemical vapor deposition (spray CVD) processes of a special type have been investigated for use in making CuInS_2 absorber layers of thin-film solar photovoltaic cells from either of two subclasses of precursor compounds: $[(\text{PBu}_3)_2\text{Cu}(\text{SEt})_2\text{In}(\text{SEt})_2]$ or $[(\text{PPh}_3)_2\text{Cu}(\text{SEt})_2\text{In}(\text{SEt})_2]$ {where Bu, Et, and Ph signify butyl, ethyl, and phenyl groups, respectively}. CuInS_2 is a member of the class of chalcopyrite semiconductors described in the immediately preceding article. $[(\text{PBu}_3)_2\text{Cu}(\text{SEt})_2\text{In}(\text{SEt})_2]$ and $[(\text{PPh}_3)_2\text{Cu}(\text{SEt})_2\text{In}(\text{SEt})_2]$ are members of the class of single-source precursors also described in the preceding article.

In a spray CVD process of this type, a room-temperature solution containing the precursor compound is first ultrasonically nebulized. The resulting aerosol is swept into a two-zone reactor by a flow of argon, which serves as a nonreactive carrier gas. In the reactor, the aerosol first encounters the evaporation zone, which is a warm zone wherein the solvent and precursor evaporate. The resulting mixture of gases then enters the deposition zone, which is a hot zone wherein the precursor decomposes and the semiconductor film grows on a substrate as in conventional CVD.

Spray CVD affords a combination of the most desirable features (but without

the major difficulties) of metalorganic CVD and spray pyrolysis. These desirable features include growth of the film in an inert atmosphere, capability for deposition on a large area, laminar flow over the substrate, and storage and delivery of the precursor from a cool solution reservoir. The last-mentioned feature is especially advantageous in that it can prevent premature decomposition of a thermally labile precursor.

Two different spray CVD processes of this type have been tested in experiments thus far. In one process, a horizontal hot-wall reactor was used; in the other process, a vertical cold-wall reactor was used (see figure). In each process, the flow rate of argon was typically about 4 L/min. For the horizontal hot-wall re-



A Horizontal Hot-Wall and a Vertical Cold-Wall Reactor have been used in experiments on spray CVD for deposition of thin CuInS_2 films.

actor, the aerosol was generated by use of an ultrasonic plate nebulizer excited at a frequency of 2.5 MHz; for the vertical-cold-wall reactor, a syringe pump delivered the solution at a rate of 1.5 mL/min to the nebulizer, wherein the aerosol was generated by use of an atomizing ultrasonic nozzle excited at a frequency of 120 kHz. In the horizontal hot-wall reactor, the portion of the wall in the evaporation zone was heated to a temperature of 130 °C, while the portion of the wall in the deposition zone was

heated to about 400 °C. In the vertical cold-wall reactor, as its name suggests, the wall was not heated; instead, the substrate was heated to 400 °C.

The CuInS₂ films produced in the experiments have been characterized by x-ray diffraction, scanning electron microscopy, energy-dispersive spectroscopy, and four-point-probe electrical tests. The results of these tests have provided some guidance for refinement of the spray CVD processes and for annealing and possibly other post-process steps to im-

prove the quality of the deposited CuInS₂ films.

This work was done by Kulbinder K. Banger, Jerry Harris, Michael H. Jin, and Aloysius Hepp of Glenn Research Center. Further information is contained in a TSP (see page 1).

Inquiries concerning rights for the commercial use of this invention should be addressed to NASA Glenn Research Center, Innovative Partnerships Office, Attn: Steve Fedor, Mail Stop 4-8, 21000 Brookpark Road, Cleveland, Ohio 44135. Refer to LEW-17447-1.

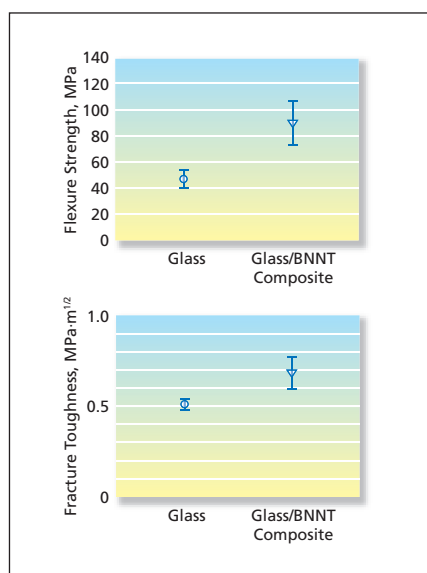
Glass/BNNT Composite for Sealing Solid Oxide Fuel Cells

Boron nitride nanotubes contribute to strength and fracture toughness.

John H. Glenn Research Center, Cleveland, Ohio

A material consisting of a barium calcium aluminosilicate glass reinforced with 4 weight percent of boron nitride nanotubes (BNNTs) has shown promise for use as a sealant in planar solid oxide fuel cells (SOFCs). The composition of the glass in question in mole percentages is 35BaO + 15CaO + 5Al₂O₃ + 10B₂O₃ + 35SiO₂. The glass was formulated to have physical and chemical properties suitable for use as a planar-SOFC sealant, but has been found to be deficient in one aspect: it is susceptible to cracking during thermal cycling of the fuel cells. The goal in formulating the glass/BNNT composite material was to (1) retain the physical and chemical advantages that led to the prior selection of the barium calcium aluminosilicate glass as the sealant while (2) increasing strength and fracture toughness so as to reduce the tendency toward cracking.

In preparation for tests, panels of the glass/BNNT composite were hot pressed and machined into test bars. Properties of the test bars, including four-point flexure strength, modulus of elasticity, mi-



Flexure Strength and Fracture Toughness of the glass and the glass/BNNT composite are compared here, with error bars signifying one standard deviation.

crohardness, and density were determined. In addition, fracture toughness was measured by the single-edge V-notch-beam method. Among the conclu-

sions drawn from the results of the tests were that the flexure strength and fracture toughness of the glass/BNNT composite specimens were greater than those of neat glass specimens by amounts of about 90 percent and about 35 percent, respectively (see figure). It was further concluded that these increases would greatly prolong the lifetimes of SOFC seals, yet there would be little adverse effect on sealing behavior of the glass because the relatively small concentration of BNNTs needed to obtain these increases would not cause much change in the viscosity of the composite sealant material.

This work was done by Narottam P. Bansal and Janet B. Hurst of Glenn Research Center and Sung R. Choi of the University of Toledo. Further information is contained in a TSP (see page 1).

Inquiries concerning rights for the commercial use of this invention should be addressed to NASA Glenn Research Center, Innovative Partnerships Office, Attn: Steve Fedor, Mail Stop 4-8, 21000 Brookpark Road, Cleveland, Ohio 44135. Refer to LEW-18094-1



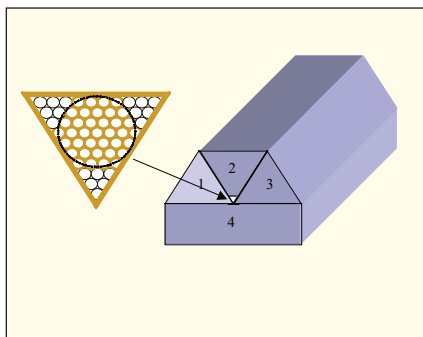
A Method of Assembling Compact Coherent Fiber-Optic Bundles

The method is based on hexagonal close packing.

NASA's Jet Propulsion Laboratory, Pasadena, California

A method of assembling coherent fiber-optic bundles in which all the fibers are packed together as closely as possible is undergoing development. The method is based straightforwardly on the established concept of hexagonal close packing; hence, the development efforts are focused on fixtures and techniques for practical implementation of hexagonal close packing of parallel optical fibers.

The figure depicts salient aspects of one such technique and fixture that may be appropriate for assembling a relatively narrow bundle in which all the fibers are known to be of the same diameter, but the diameter is not known precisely. The positions and ori-



Two of the Three Clamping Blocks are positioned and oriented, relative to the third block, to squeeze the optical fibers into an equilateral triangular cross section. Then the fibers and clamping blocks are fixed in a housing by use of an epoxy.

entations of the three blocks are adjusted to accommodate the diameter and to push the fibers together into an equilateral triangular cross section that enforces the required regular hexagonal arrangement. Once the fibers have been clamped together as shown in the upper part of the figure, the bundle and its clamping blocks could be fixed in the desired position in a housing by use of an epoxy.

This work was done by Stefan Martin, Duncan Liu, Bruce Martin Levine, Michael Shao, and James Wallace of Caltech for NASA's Jet Propulsion Laboratory. Further information is contained in a TSP (see page 1).
NPO-30913

Manufacturing Diamond Under Very High Pressure

Pure or doped diamond is crystallized from molten carbon and in solid state.

Marshall Space Flight Center, Alabama

A process for manufacturing bulk diamond has been made practical by the invention of the High Pressure and Temperature Apparatus capable of applying the combination of very high temperature and high pressure needed to melt carbon in a sufficiently large volume. The rate of growth achievable in this process is about ten times the rate achievable in older processes. Depending on the starting material and temperature-and-pressure schedule, this process can be made to yield diamond in any of a variety of scientifically and industrially useful forms, including monocrystalline, polycrystalline, pure, doped, and diamond composite. (Doping makes it possible to impart desired electrical and optical properties, including semiconductivity and color.) The process can also be used to make cubic boron nitride.

The difficulties of manufacturing diamond can be summarized as follows:

- Diamond can be made from dispersed phases of carbon (in which carbon atoms are surrounded by atoms of other ele-

ments or compounds), but the rate of growth is low and the product is impure.

- Diamond crystals can be grown from molten carbon at a high rate, but carbon does not melt at ambient pressure.
- In the range of temperature high enough for forming diamond at a high rate, diamond transforms into graphite if the pressure is not high enough.

The apparatus includes a reaction cell wherein a controlled static pressure as high as 20 GPa and a controlled temperature as high as 5,000 °C can be maintained. A precursor material that consists of either pure or doped diamond powder is placed in a graphite crucible that, in turn, is placed in the reaction cell. The pressure in the cell is increased at ambient temperature, then the temperature is increased. Next, the cell is cooled, at a controlled rate, to a lower temperature where carbon crystallizes. If this controlled cooling is sufficiently slow, single-crystal diamond is formed; faster cooling causes the formation of

polycrystalline diamond. After crystallization, the reaction cell is cooled and depressurized to room temperature and pressure, the reaction cell is extracted from the apparatus, the graphite crucible is extracted from the reaction cell, then the crucible is broken to extract the bulk diamond.

The one major disadvantage of this process is that because of the difficulty of maintaining the combination of high temperature and pressure, the apparatus and process are expensive and the volume of the crucible must be limited. Nevertheless, the process is scalable, and the economic value of the tailored diamond products may justify the cost of scaling the apparatus up to larger production quantities. Working prototype is available at Diamond Materials Inc. facility and can be visited.

This work was done by Oleg Voronov of Diamond Materials, Inc. for Marshall Space Flight Center. Further information is contained in a TSP (see page 1).



Ring-Resonator/Sol-Gel Interferometric Immunosensor

Light would make multiple passes through the sensing volume.

NASA's Jet Propulsion Laboratory, Pasadena, California

A proposed biosensing system would be based on a combination of (1) a sensing volume containing antibodies immobilized in a sol-gel matrix and (2) an optical interferometer having a ring resonator configuration. The antibodies

target the antigen species of interest.

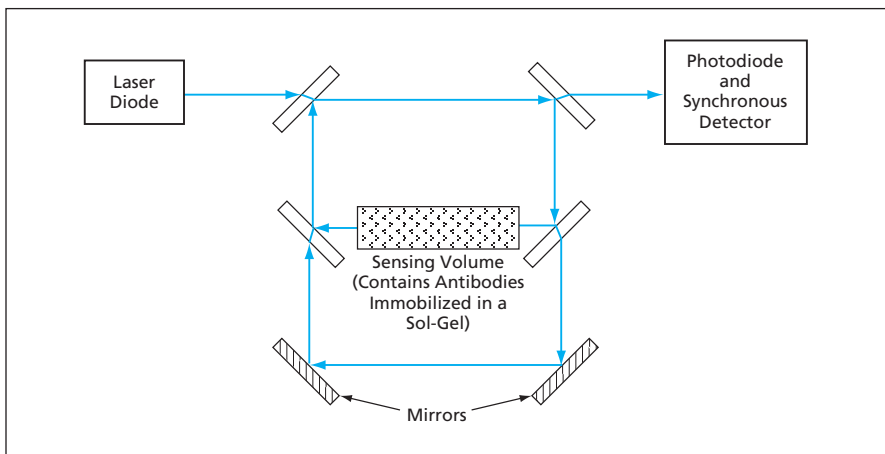
The basic principle of using interferometry to detect antibody-antigen binding is not new in itself. However, the prior implementation of this principle has involved the use of a Mach-

ferometer configuration, there would be two interferometer arms with coupled optical paths. One of the optical paths would pass through the sensing volume; the other optical path would not pass through the sensing volume (see figure). Interference between light beams in the two interferometer arms would be characterized by a phase difference proportional to the change in the index of refraction of the sensing volume. The phase difference would result in a change in the interferometer output intensity measured by use of a photodiode. A synchronous detector could be used to increase sensitivity.

The ring resonator/interferometer could be built by use of traditional bulk optical components or fabricated as a unit by standard silicon-fabrication techniques. Inasmuch as a sol-gel precursor can be poured into a mold, an etched recess in a planar waveguide or other structures could be used as the sensing volume.

This work was done by Gregory Bearman and David Cohen of Caltech for NASA's Jet Propulsion Laboratory. Further information is contained in a TSP (see page 1).

This invention is owned by NASA, and a patent application has been filed. Inquiries concerning nonexclusive or exclusive license for its commercial development should be addressed to the Patent Counsel, NASA Management Office-JPL. Refer to NPO-30807.



A Ring Resonator/Interferometer would include a sensing volume on one of its optical paths. Binding of antigens to antibodies would cause a change in the index of refraction of the sensing volume leading to a change in the photodiode output.

would be specific to an antigen species that one seeks to detect. The binding of the antigens to the immobilized antibodies would change the index of refraction of the sensing volume, which would be mounted in one of the interferometer arms. The interferometer would measure the change in the index of refraction, thereby indirectly measuring the concen-

tration of the antigen species of interest. Zehnder interferometer, which affords only a single pass of light through the sensing volume. In the ring resonator of the proposed system, light would make multiple passes through the sensing volume, affording greater interaction length and, hence, greater antibody-detection sensitivity.

In one proposed ring-resonator/inter-

Compact Fuel-Cell System Would Consume Neat Methanol

Size, mass, and parasitic power consumption would be reduced.

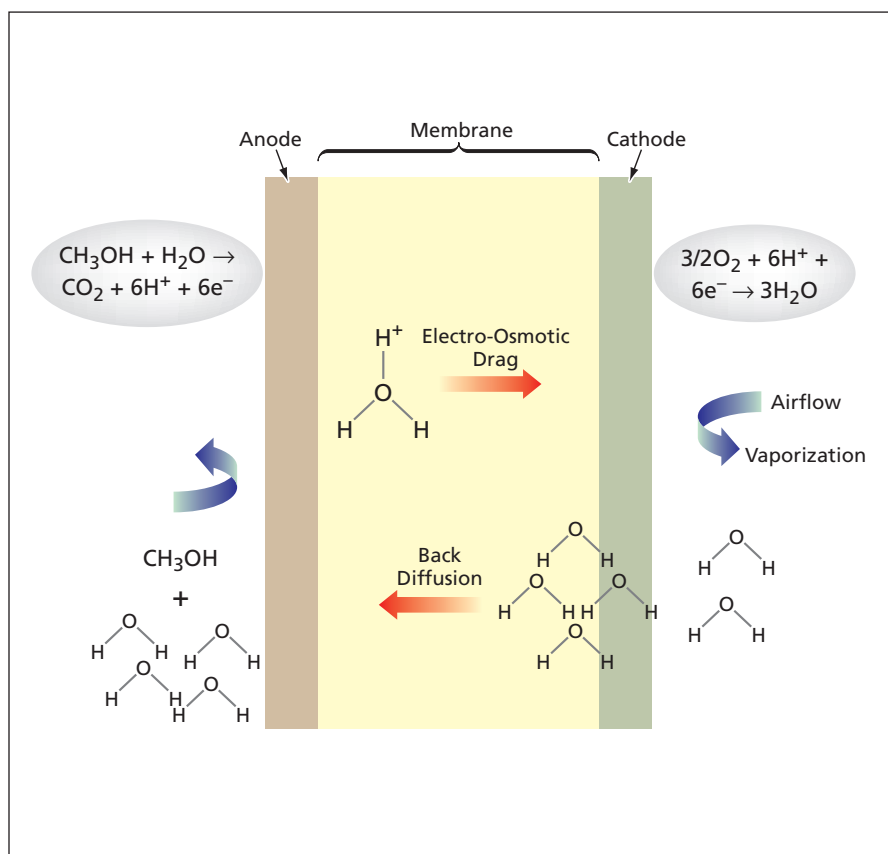
NASA's Jet Propulsion Laboratory, Pasadena, California

In a proposed direct methanol fuel-cell electric-power-generating system, the fuel cells would consume neat methanol, in contradistinction to the dilute aqueous methanol solutions consumed in prior direct methanol fuel-cell systems. The design concept of the proposed fuel-cell system takes advantage of (1) electro-osmotic drag and diffusion

processes to manage the flows of hydrogen and water between the anode and the cathode and (2) evaporative cooling for regulating temperature. The design concept provides for supplying enough water to the anodes to enable the use of neat methanol while ensuring conservation of water for the whole fuel-cell system. By rendering unnecessary some of the auxil-

iary components and subsystems needed in other direct methanol fuel-cell systems for redistributing water, diluting methanol, and regulating temperature, this fuel-cell design would make it possible to construct a more compact, less massive, more energy-efficient fuel-cell system.

In a typical prior direct methanol fuel-cell system, neat methanol is stored in a



The **Transport Processes** involved in the operation of a direct methanol fuel cell figure prominently in the proposed design.

container and then diluted with water to a concentration between 2 and 3 percent before it is introduced into the fuel-cell stack. Water for dilution is gathered from the cathode side of the fuel-cell stack. The fuel solution is recirculated, the fuel solution entering the anodes is monitored by use of a methanol sensor, and, in response to the sensor reading, methanol is added to the solution as needed to maintain the required concentration. The collection of water, the dilution of methanol, the control of concentration, and the circulation of the fuel solution entail the use of several pumps and control subsystems, and substantial electrical energy is consumed in operating the pumps and control subsystems. These auxiliary components and subsystems typically contribute about half of the overall volume and mass and at least half of the parasitic energy consumption of the system.

The figure schematically depicts the transport processes involved in the operation of a direct methanol fuel cell (whether of prior or proposed design). Methanol is oxidized to protons and carbon dioxide at the anode, and oxygen is reduced to water at the cathode. As protons migrate from the anode to the cathode through a proton-con-

ducting membrane that is part of a membrane/electrode assembly, water is transported along with them by electro-osmotic drag: in other words, water molecules associated with the protons are dragged along with the protons. Air flowing over the cathode evaporates some of the water. However, some of the water tends to diffuse back toward the anode because the concentration of water at the cathode exceeds the concentration of water in the methanol-water solution at the anode (this diffusion is hereafter denoted "back diffusion"). Water is consumed at the anode by the oxidation of methanol, and water is produced at the cathode by reduction of oxygen.

The rate of consumption of water at the anode is proportional to the electric-current density. The rate of electro-osmotic drag of water from the anode to the cathode is determined by the electric-current density and a drag coefficient that amounts to about 3 molecules of water per proton. The rate of production of water in the chemical reaction at the cathode is also proportional to the electric-current density. The rate of flow of air over the cathode, the temperature of the cell, and the absolute humidity of

the air at that temperature determine the rate of evaporation. The gradient of concentration of water between the anode and the cathode and the diffusion coefficient of water in the membrane/electrode composite determine the rate of back diffusion.

In a fuel cell of prior design, the rate of back diffusion is insufficient, necessitating the use of pumps to return water from the cathode to the anode side. The proposed fuel-cell design concept provides for enhancement of the rate of back diffusion through enhancement of the gradient of concentration of water between the anode and the cathode, thereby eliminating the need for the pumps and controls heretofore needed for this purpose.

The enhancement of the gradient of concentration of water would be effected, nearly independently of the electric-current density, through appropriate choice of the concentration of methanol, the porosity of the electrodes, the thickness of the membrane, the operating temperature, and the stoichiometric rate of flow of air. For any given set of values of these parameters, there would be an electric-current density at which water balance would be achieved. Therefore, a membrane/electrode assembly capable of supporting any desired value of electric-current density and maintaining water balance could be designed for use in a fuel cell without need for pumps or other components for dilution or for redistribution of water.

An important consideration in the design concept is that an uncontrolled excess of neat methanol at the anode would cause swelling of the membrane. Therefore, the rate of delivery of methanol must be such that only a small quantity of methanol reaches the anode and that the entire quantity of delivered methanol be utilized within the anode, so that no appreciable quantity of neat methanol can reach the surface of the membrane. The full utilization of methanol could be achieved if the anode structure were made sufficiently porous and thick: such a structure would ensure that the residence time for methanol was adequate for complete consumption of ethanol within the anode structure. The porous anode structure would contain enough proton-conducting polymer material to form conducting paths for protons and water molecules, yet would have enough tortuosity to afford sufficient residence time. The anode structure would include layers having various proton-conducting-polymer contents so

that the desired level of utilization could be achieved. The design choice of thickness and porosity of the anode would depend on the planned rate of delivery of methanol and on whether the methanol were to be delivered directly in purely liquid form, delivered directly in aerosol form, or delivered in purely liquid form through a diffusion barrier.

The design must provide for removal of excess heat. In a fuel cell of prior design, one can utilize the circulation of the dilute fuel solution to remove heat on the anode side and evaporative cool-

ing on the cathode side. In the absence of fuel-solution circulation in the proposed design and without further modification, only evaporative cooling would be available. Under most conditions, evaporative cooling alone may not suffice, so that it may be necessary to add cooling fins to the fuel-cell stack.

This work was done by Sekharipuram Narayanan, Andrew Kindler, and Thomas Valdez of Caltech for NASA's Jet Propulsion Laboratory. Further information is contained in a TSP (see page 1).

In accordance with Public Law 96-517,

the contractor has elected to retain title to this invention. Inquiries concerning rights for its commercial use should be addressed to:

*Innovative Technology Assets Management
JPL*

Mail Stop 202-233

4800 Oak Grove Drive

Pasadena, CA 91109-8099

(818) 354-2240

E-mail: iaoffice@jpl.nasa.gov

Refer to NPO-41661, volume and number of this NASA Tech Briefs issue, and the page number.



Σ Algorithm Would Enable Robots to Solve Problems Creatively

A control architecture is based on hypotheses concerning natural intelligence.

Lyndon B. Johnson Space Center, Houston, Texas

A control architecture and algorithms to implement the architecture have been conceived to enable a robot to learn from its experiences and to combine knowledge gained from prior experiences in such a way as to be able to solve new problems. The architecture is an abstraction of an interacting system of relatively simple components that, when properly interconnected, should enable the spontaneous emergence of behaviors from the complete system that would not necessarily be expected from the individual components. These emergent behaviors should enable a robot to interact robustly and intelligently with a complex, dynamic environment.

Departing from the customary approach to artificial intelligence, the theoretical foundation of this architecture includes a hypothesis that has gained some acceptance in research on natural intelligence in animals. Stated succinctly, the hypothesis is that intelligence requires embodiment, situatedness, development, and interaction. Applied to a computer, the hypothesis states that to be able to develop intelligence, a computer must be able to, among other things, manipulate the environment and sense the results; in other words, the computer must be equipped with a robotic interface with the physical world. A related hypothesis is that sensory-motor coordination forms the basis for intelligent behavior, and, hence, intelligence. This follows from the demonstrated ability of sensory-motor coordination information to self-organize into categories.

The architecture represents a set of parallel distributed computational modules (software objects) that communicate with each other through message passing. The principal objects loosely correspond to the (presumed) common computational modules of mammalian brains. A set of sensory processing modules continually updates a spatio-temporally indexed short-term memory structure denoted the sensory ego-sphere

(SES). Depending on the task context, an attentional mechanism determines the saliency of incoming sensory information. In response to changes in the state of motion of the robot, the time series of sensory information is partitioned into episodes. Episodes are encoded in vector form and stored in a database, denoted the database associative memory (DBAM), that comprises the long-term memory of the robot.

The DBAM has the implicit mathematical structure of a linear vector space that is constructed as the direct sum of three subspaces. One subspace encodes a change in motor state (a motor event). Another subspace encodes the state of the sensors immediately prior to the motor event — in other words, the sensory preconditions of the motor event. The third subspace encodes the sensory state subsequent to the motor event (sensory post-conditions). The vectors in the DBAM and the external events from which they are formed are called sensory-motor coordination (SMC) events.

Several research projects have demonstrated that over time, as a robot senses and acts, clusters form within a vector space of SMC descriptors. Categories emerge. Thus, it becomes possible to select an exemplar that describes an equivalence class of SMC events. The encoding of SMC events as motor events with sensory preconditions and sensory post-conditions makes it possible to use simple vector-space distances as measures of dissimilarity or similarity of complete SMC events. Vector-space distances can also serve as measures of dissimilarity or similarity between the sensory post-conditions of one event and the sensory preconditions of another.

The architecture utilizes a control strategy, called topological action mapping, that appears to be employed by mammals to achieve specific goals. In this architecture, action maps are implemented by a spreading activation network (SAN). (A SAN is one of a particu-

lar class of graph traversal algorithms that selects optimal paths.) For each goal to be reached by the robot, there corresponds an SMC event. Moreover, the current state of the robot is indicated by an SMC event. Given the goal event, the SAN searches through the DBAM, matching its sensory preconditions to the sensory post-conditions of other events. The search is constrained by a number of global state variables and previously formed linkages. Upon finding a sufficiently close match, the SAN iterates the search until the current state is reached. The current motor state (hence, the current behavior) is maintained until the sensory post-conditions trigger a change of state. Thus, the robot proceeds through a sequence of behaviors until the goal is reached.

One key aspect of this architecture is that the robot cannot be programmed through conventional means: it must be taught to perform tasks, either through direct control or by example. The robot must practice each task several times to enable the formation of clusters of SMC events and to learn the sequences of these events. Such repetition enables the robot to perform the task later, without supervision. However, this does not, in itself, enable creative problem solving.

To be able to solve problems creatively, the robot must engage in a process analogous to dreaming. After intervals of continuous motor activity, the robot performs computations in which it plays back data on recently performed sequences of tasks. SMC events are compared quasi-randomly to other events in the DBAM. If the sensory post-conditions of a given event are sufficiently similar to the sensory precondition of another event, links are formed between them. Such a link is formed, even if the two behaviors have never occurred in sequence before. This link gives the robot a new possible behavior transition that it could make, given the appropriate sensory trigger. Thus, the robot learns to an-

ticipate possible sequences of events and learns strategies for the solving of problems that it has not encountered but that could occur.

The architecture is still undergoing development. An SES has been implemented in the NASA Robonaut (a developmental anthropomorphic robot intended to serve as an astronaut's assistant). Production-quality software to implement the architecture has not

yet been written. A major problem in writing this software is that of efficient representation of sensory data in vector spaces.

This work was done by Alan Peters of Vanderbilt University for Johnson Space Center.

In accordance with Public Law 96-517, the contractor has elected to retain title to this invention. Inquiries concerning rights for its commercial use should be addressed to:

*Christopher D. McKinney, Director
Office of Technology Transfer
and Enterprise Development
Vanderbilt University*

*1207 17th Avenue South, Suite 105
Nashville, TN 37212*

Phone: (615) 343-2430

E-mail: chris.mckinney@vanderbilt.edu

*Refer to MSC-23489, volume and number
of this NASA Tech Briefs issue, and the
page number.*

Hypothetical Scenario Generator for Fault-Tolerant Diagnosis

This is a means of performing diagnostic reasoning when data are missing.

NASA's Jet Propulsion Laboratory, Pasadena, California

The Hypothetical Scenario Generator for Fault-tolerant Diagnostics (HSG) is an algorithm being developed in conjunction with other components of artificial-intelligence systems for automated diagnosis and prognosis of faults in spacecraft, aircraft, and other complex engineering systems. By incorporating prognostic capabilities along with advanced diagnostic capabilities, these developments hold promise to increase the safety and affordability of the affected engineering systems by making it possible to obtain timely and accurate information on the statuses of the systems and predicting impending failures well in advance.

Prognosis is tightly coupled with diagnosis. The simplest approach to prognosis by an artificial-intelligence system involves the use of a diagnostic engine in a controlled feedback loop to project from the current state of the affected engineering system to future states that are elements of scenarios that are discovered hypothetically. A hypothetical-scenario generator is a key element of this

approach. A hypothetical-scenario generator accepts, as its input, information on the current state of the engineering system. Then, by means of model-based reasoning techniques, it returns a disjunctive list of fault scenarios that could be reached from the current state.

The HSG is a specific instance of a hypothetical-scenario generator that implements an innovative approach for performing diagnostic reasoning when data are missing. The special purpose served by the HSG is to (1) look for all possible ways in which the present state of the engineering system can be mapped with respect to a given model and (2) generate a prioritized set of future possible states and the scenarios of which they are parts. The HSG models a potential fault scenario as an ordered disjunctive tree of conjunctive consequences, wherein the ordering is based upon the likelihood that a particular conjunctive path will be taken for the given set of inputs. The computation of likelihood is based partly on a numerical ranking of the degree of completeness

of data with respect to satisfaction of the antecedent conditions of prognostic rules. The results from the HSG are then used by a model-based artificial-intelligence subsystem to predict realistic scenarios and states.

To avoid the need to create special models to generate hypothetical scenarios, the HSG uses the same model that is used to perform fault-detection and other diagnostic functions but interprets the results generated by the model in a manner unique to the generation of hypothetical scenarios. An important additional advantage of this approach is that a future state can be diagnosed by the same model as that used to diagnose the current state.

This work was done by Mark James of Caltech for NASA's Jet Propulsion Laboratory. Further information is contained in a TSP (see page 1).

The software used in this innovation is available for commercial licensing. Please contact Karina Edmonds of the California Institute of Technology at (626) 395-2322. Refer to NPO-42516.



Books & Reports

Smart Data Node in the Sky

A document discusses the physical and engineering principles affecting the design of the Smart Data Node in the Sky (SDNITS) — a proposed Earth-orbiting satellite for relaying scientific data from other Earth-orbiting satellites to one or more ground station(s). The basic concept of the SDNITS is similar to that of NASA's Tracking Data Relay Satellite System (TDRSS). However, the SDNITS would satisfy the needs of the next generation of Earth-observing satellite missions, including, notably, the need to relay data at much higher rates — of the order of 10 Gb/s versus ≤ 400 Mb/s for the TDRSS.

The document characterizes the problem of designing the telecommunication architecture of the SDNITS as consisting of two main parts: (1) finding the most advantageous orbit for the SDNITS to gather data from the scientific satellites and relay the data to the ground, taking account of such factors as visibility and range; and (2) choosing a telecommunication architecture appropriate for the intended relay function. The design of the SDNITS would incorporate technological advances — especially in the field of high-rate data transmission — that have occurred during the three decades since the TDRSS was designed.

This work was done by Faiza Lansing and Anil Kantak of Caltech for NASA's Jet Propulsion Laboratory. Further information is contained in a TSP (see page 1). NPO-30904

Pseudo-Waypoint Guidance for Proximity Spacecraft Maneuvers

A paper describes algorithms for guidance and control (G&C) of a spacecraft maneuvering near a planet, moon, asteroid, comet, or other small astronomical body. The algorithms were developed following a model-predictive-control approach along with a convexification of the governing dynamical equations, control constraints, and trajectory and state constraints. The open-loop guidance problem is solved in advance or in real time by use of the pseudo-waypoint generation (PWG) method, which is a blend

of classical waypoint and state-of-the-art, real-time trajectory-generation methods. The PWG method includes satisfaction of required thruster silent times during maneuvers. Feedback control is implemented to track PWG trajectories in a manner that guarantees the resolvability of the open-loop-control problem, enabling updating of G&C in a provably robust, model-predictive manner. Thruster firing times and models of the gravitational field of the body are incorporated into discretized versions of the dynamical equations that are solved as part of an optimal-control problem to minimize consumption of fuel or energy. The optimal-control problem is cast as a linear matrix inequality (specifically a second-order cone program), then solved through semi-definite-programming techniques in a computationally efficient manner that guarantees convergence and satisfaction of constraints.

This work was done by Ahmet Açikmeşe and John M. Carson III of Caltech for NASA's Jet Propulsion Laboratory. Further information is contained in a TSP (see page 1).

The software used in this innovation is available for commercial licensing. Please contact Karina Edmonds of the California Institute of Technology at (626) 395-2322. Refer to NPO-42753.

Update on Controlling Herds of Cooperative Robots

A document presents further information on the subject matter of "Controlling Herds of Cooperative Robots" (NPO-40723), *NASA Tech Briefs*, Vol. 30, No. 4 (April 2006), page 81. To recapitulate: A methodology for controlling a herd of cooperative and autonomous mobile robots exploring the surface of a remote planet or moon (specifically, Titan or Titan-like) is undergoing development. The proposed configuration of mobile robots consists of a blimp and a herd of surface sondes. The blimp is the leader of the herd, and it commands the other robots to move to locations on the surface or below the surface to conduct science operations. Once a target is chosen, the sondes cooperatively aim sensors at the target to maximize scientific return. This hierarchical and cooperative behavior is necessary in the face of such unpredictable factors as terrain obstacles and uncertainties in

the model of the environment.

This document describes the cooperation architecture and the estimation algorithm. Dynamical and kinematical models of the blimp and surface sondes are derived, and a robust guidance and control algorithm, based on a potential-field mathematical model, is developed. This guidance-and-control algorithm can compute actuator forces needed for moving the surface sondes across the terrain while avoiding hazards and collisions with each other and at the same time remaining within communication range with the blimp.

The document describes the results of the computational simulations of a one-blimp, three-surface-sonde herd in various operational scenarios, including sensitivity studies as a function of distributed communication and processing delays between the sondes and the blimp. From results of the simulations, it is concluded that the methodology is feasible, even if there are significant uncertainties in the dynamical models.

This work was done by Marco Quadrelli and Johnny Chang of Caltech for NASA's Jet Propulsion Laboratory. Further information is contained in a TSP (see page 1).

The software used in this innovation is available for commercial licensing. Please contact Karina Edmonds of the California Institute of Technology at (626) 395-2322. Refer to NPO-35031.

Simulation and Testing of Maneuvering of a Planetary Rover

A report discusses the development of a computational model of a Mars Explorer Rover maneuvering across terrain under varying conditions. The model is used to increase understanding of the rover dynamics. Increased understanding is helpful in planning further tests and in extending the operational range of the rover to terrain conditions that would otherwise have to be avoided in a conservative approach. The model is implemented within MSC.ADAMS®, a commercial suite of computer programs for simulating a variety of automotive and aeronautical mechanical systems. Following its initial formulation, the model has been successively refined in an iterative

process of simulation, testing on simulated terrain, correlation of simulation results with test results, and adjustment of model parameters to increase degrees of matching between simulation and test results. In particular, three aspects of the model have been refined, as follows:

- Wheel radius, which was set to cancel

effects of cleats, and of compliance and roughness of the ground surface;

- A submodel of friction between the wheels and a high-friction mat used in the tests; and
- A submodel of internal and external power losses that includes no-load power consumed by wheel mechanisms and nominal rolling resistance.

This work was done by Gary Ortiz and Randal Lindemann of Caltech for NASA's Jet Propulsion Laboratory. Further information is contained in a TSP (see page 1).

The software used in this innovation is available for commercial licensing. Please contact Karina Edmonds of the California Institute of Technology at (626) 395-2322. Refer to NPO-42547.

